Carbonate in Synthetic and Biological Apatites

M E Fleet[1] and X Liu[2]

ABSTRACT

The crystal chemistry of carbonate in Ca apatites, including Na-free and Na-bearing hydroxylapatite (CHAP) and Na-bearing fluorapatite (CFAP) and chlorapatite (CCLAP), has been investigated by Fourier transform infrared (FTIR) spectroscopy and single-crystal X-ray structure, using crystals synthesised from carbonate-rich melts at 1 GPa, 1400 - 1000°C. The carbonate ion substitutes for both the X (OH, F, Cl) anion species in the apatite channel (type A carbonate) and the phosphate group (type B carbonate). The type A carbonate ion is oriented in the channel with two oxygen atoms close to the *c*-axis, and the type B carbonate ion is located close to the sloping faces of the substituted phosphate tetrahedron, with details varying with composition series. Sodium promotes the uptake of type B carbonate and also has a profound effect on FTIR spectra. Crystal compositions correspond approximately to the substitution formula $Ca_{10-(y+z)}Na_y\,\square_z[(PO_4)_{6-(y+2z)}(CO_3)_{y+2z}][X_{2-2x}(CO_3)_x]$, with $x \approx y$ up to 1.0 and $z \approx 0.0$ for CHAP, $x \approx y \approx 4z \approx 0.4$ for CCLAP, and $x \approx y \approx 2z \approx 0.1$ for CFAP, for equivalent conditions of synthesis. The sodium cation and A and B carbonate ion defects are locally coupled in all three composition series to facilitate charge compensation and minimise the effects of spatial accommodation. Synthetic Na-bearing type A-B CHAP with $x \approx y \approx 0.5$ has a similar chemical composition and FTIR spectrum to biological apatite.

INTRODUCTION

The calcium phosphate apatites [$Ca1_4Ca2_6(PO_4)_6X_2$; with X = F, OH, Cl, O, etc] (eg Pan and Fleet, 2002) have importance in both geochemistry and biology. Apatites sequester phosphorus, rare earth elements, actinides and volatile elements in the Earth's crust and mantle (eg O'Reilly and Griffin, 2000; Pan and Fleet, 2002; Harlov, Foerster and Nijland, 2002). Also, fluorapatite is a practical host for the containment of high-level nuclear waste, as evidenced by its occurrence in the natural reactor at Oklo, Gabon (eg Bros *et al*, 1996). Within the biosphere, carbonate-bearing hydroxylapatite (presently abbreviated as CHAP) is by far the most important biomineral, accounting for up to about 65 wt per cent of cortical bone and 97 wt per cent of dental enamel (Elliott, 2002; Wopenka and Pasteris, 2005). Fluoride hosted by CHAP is the important anticaries component of dental enamel (Brudevold, Gardner and Smith, 1956), and CHAP and carbonated fluorapatite (CFAP; also francolite) are the dominant minerals in phosphorites (McClellan and Lehr, 1969).

The structural role of carbonate in hydroxylapatite and fluorapatite has been investigated extensively by X-ray powder and single-crystal and neutron powder diffraction methods (eg Elliott, 1994; Suetsuga *et al*, 2000; Ivanova *et al*, 2001; Wilson, Elliot and Dowker, 1999; Wilson *et al* 2004; Wilson, Dowker and Elliot, 2006; Leventouri *et al*, 2000, 2001; Antonakos, Liarokapis and Leventouri, 2007), as well as by infrared, Raman and nuclear magnetic resonance spectroscopy (eg Elliott, 1964; Bonel, 1972; LeGeros *et al*, 1969; Rey *et al*, 1989, 1991; Kim, Rey and Gilmcher, 1996; Cho, Wu and Ackerman, 2003; Mason, Kozlowski and Phillips, 2007). It has been established that the carbonate ion can be accommodated either in the *c*-axis structural channel or as a substituent for the phosphate group: the former carbonate is known as type A and the latter as type B. However, the structural details and estimation of the proportion of types A and B carbonate (in A-B apatites) have remained controversial. Structure analysis by diffraction methods has been frustrated by several factors, including:

- the limited substitution of carbonate (especially of type B carbonate),
- small (nanoscale) crystal size of biological and inorganically precipitated apatite and of francolite from phosphorites,
- poor crystallinity, and
- weak and overlapped electron densities of carbonate atoms.

In this paper we review recent studies on the accommodation of carbonate in Na-free CHAP and Na-bearing CHAP, CFAP and carbonate chlorapatite (CCLAP) using the X-ray single-crystal structure method and crystals grown from carbonate-rich melts at high pressure (Fleet and Liu, 2003, 2004, 2005, 2007a, 2008a, 2008b; Fleet, Liu and King, 2004). The crystal growth experiments were performed in a Quickpress (Depths of the Earth Co LLC) and end-loaded piston cylinder apparatus. Experimental details are given in the studies listed above. High temperature was required to yield crystals of a size suitable for X-ray structure analysis, and high pressure to confine CO_2-rich fluid and vapour. Nevertheless, we show that the crystal products, particularly of CHAP, reproduce the infrared (IR) spectra of apatite biominerals and, therefore, appear to be appropriate analogues for their overall structural features.

EXPERIMENTAL PRODUCTS

The products of the crystal growth experiments were carbonate apatite in the form of relatively large hexagonal prisms ranging up to 300 μm in size, which had evidently crystallised from the melt at the experimental temperature, and a fine-grained matrix of apatite and minor carbonates of quench origin. They were characterised by optical microscopy, powder X-ray diffraction, electron probe microanalysis, and Fourier transform infrared (FTIR) spectroscopy. Infrared spectra were obtained for both hand separated apatite crystals and bulk products using KBr pellets. Single-crystal X-ray diffraction measurements were made at room temperature and pressure with a Bruker-Nonius Kappa CCD diffractometer and graphite-monochromatised Mo $K\alpha$ X-radiation (50 kV, 32 mA, λ = 0.7107 Å). Procedures for data reduction and structure analysis are reported in Fleet and Liu (2003, 2004, 2007a, 2008a, 2008b) and Fleet, Liu and King (2004). Experimental conditions are summarised in Table 1.

The uptake of carbonate by apatite varied markedly from one composition series to another for similar conditions of synthesis (Table 1): for Na-bearing carbonate apatites, it was greatest for CHAP, with a maximum amount of 8.2 wt per cent CO_2, least for CFAP at 1.9 wt per cent, and intermediate for CCLAP at 3.4 wt per cent. Several experiments on CFAP and CCLAP were subjected to a two-stage heating in an attempt to investigate the effect of annealing temperature on the extent of carbonate substitution, but yielded inconclusive results. The uptake of carbonate was minimal for CFAP crystals grown very close to the liquidus (LM134 in Fleet and Liu, 2008a), but the excess amount of CaF_2 in the starting composition may have been a factor here in shifting crystal compositions toward the more refractory FAP end member. Correspondingly, FTIR spectra of all bulk samples consistently indicated a higher content of carbonate than separated apatite crystals from the same experiments (cf, d and c in Figure 1), reflecting the greater contribution of the low-melting component in apatite precipitated during quenching.

1. University of Western Ontario, Department of Earth Sciences, London, ON N6A 5B7, Canada. Email: mfleet@uwo.ca

2. School of Earth and Space Sciences, Peking University, Beijing 100871, China. Email: xi.liu@pku.edu.cn

TABLE 1

Synthesis experiments and amounts of Na, A and B carbonate (pfu[1]).

Apatite	Expt	T	P	EPMA	X-ray structure			FTIR[2]
		(°C)	(GPa)	Na	A	B	B/A	B/A
Na-free synthetic apatites								
CHAP	PC17	1400	3.0	-	0.0	0.17(2)	-	1.3
	PC71	1400	2.0	-	0.75	0.11(2)	0.2	0.2
	PC18	1400	3.0	-	1.08(8)[3]	0.49(2)	0.5	0.5
	PC55	1400	3.0	-	1.26(4)	0.57(2)	0.5	0.4
Na-bearing synthetic apatites								
CHAP	LM005	1200	0.5	0.87(3)	1.00(5)	0.77(3)	0.8	0.9
	LM006	1200	1.0	0.35(4)	0.52(3)	0.38(2)	0.7	0.8
CCLAP	LM169	1350	1.0	0.40(4)	0.37(3)	0.57(2)	1.5	1.5
	LM171	1350/1200[4]	1.0	0.39(3)	0.46(4)	0.58(3)	1.3	1.6[5]
	LM173	1350/1000	1.0	0.39(5)	0.42(3)	0.57(2)	1.4	1.4
CFAP	LM130	1250	1.0	0.09(3)	0.08(3)	0.23(1)	2.9	2.6
	LM136	1250	1.0	0.09(3)	0.16(3)	0.21(2)	1.3	1.2
	LM142	1350/1150	1.0	0.11(5)	0.14(3)	0.23(1)	1.6	1.5

Notes:

1. pfu is per formula unit.
2. Using ν_2 band.
3. Type A carbonate for PC18 and PC55 is A1+A2 (Fleet, Liu and King, 2004).
4. Two-stage heating; second number is final annealing temperature.
5. From bulk spectrum.

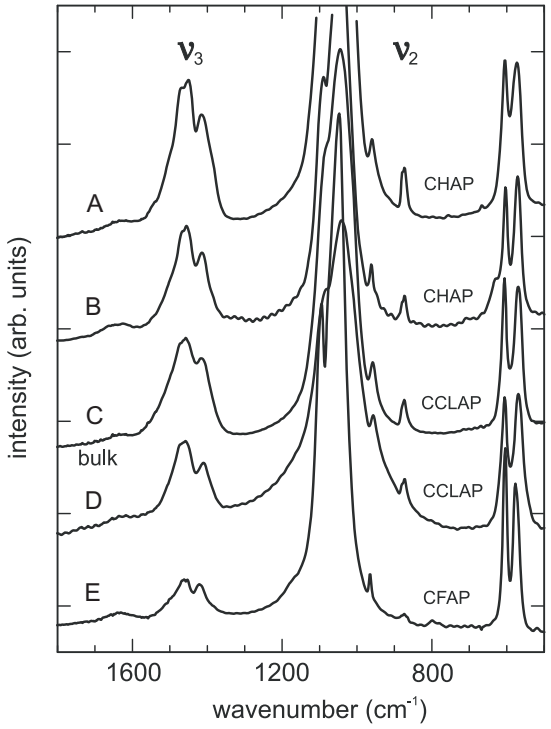

FIG 1 - Fourier transform infrared (FTIR) spectra for Na-bearing type A-B carbonate apatites synthesised at high *P-T*, identifying bands due to asymmetric stretching (ν_3) and out-of-plane bending (ν_2) of carbonate ions: (A) CHAP, LM005; (B) CHAP, LM006; (C) CCLAP, LM169 (bulk sample); (D) CCLAP, LM169; (E) CFAP, LM130. Note that the spectra for (A), (B), (D) and (E) were collected using hand-separated crystals: see text for band assignments and interpretation.

CALCIUM APATITE STRUCTURE

Calcium apatite minerals are dominantly solid solutions of hydroxylapatite [HAP; ideally $Ca_{10}(PO_4)_6(OH)_2$; Z = 1], fluorapatite [FAP; $Ca_{10}(PO_4)_6F_2$] and chlorapatite [CLAP; $Ca_{10}(PO_4)_6Cl_2$]. The natural phases all have the hexagonal space group $P6_3/m$, although pure, end-member HAP and CLAP crystallise in the monoclinic space group $P2_1/b$ (Hughes and Rakovan, 2002; White *et al*, 2005). The $P6_3/m$ structure of calcium apatites is well known. Apatite is an orthophosphate. Isolated PO_4 tetrahedra centred at z = 1/4, 3/4 are linked by Ca1 in ninefold (6+3) coordination and Ca2 in an irregular sevenfold (6+1) coordination (Figure 2). A prominent feature of the structure is the large *c*-axis channel which accommodates the X anion component (F, OH, Cl), and is defined by triclusters of Ca2 cations at z = 1/4, 3/4 (Figure 3). In fluorapatite (FAP), the F anion is located on the *c*-axis at z = 1/4, 3/4 in the centre of a tricluster of Ca cations. OH in HAP and Cl in CLAP are displaced along the *c*-axis and have split atom positions with occupancy of 0.5: the hydroxyl oxygen is at $z = \pm$ (0.198, 0.302) and the much larger Cl anion is displaced further at $z = \pm$ (0.432, 0.068) (Hughes, Cameron and Crowley, 1989). Thus, the coordination of the X anion is equilateral triangular in FAP but near octahedral in CLAP.

RESULTS AND DISCUSSION

Detection of carbonate by Fourier transform infrared spectroscopy

The substitution of carbonate into apatite is most readily detected by Fourier transform infrared (FTIR) spectroscopy (eg Figures 1 and 4), although this method can yield ambiguous results when used to determine the proportion of type A and B carbonate ions. The literature on the application of infrared spectroscopy to carbonate in apatite is voluminous, with Elliott (1964), LeGeros

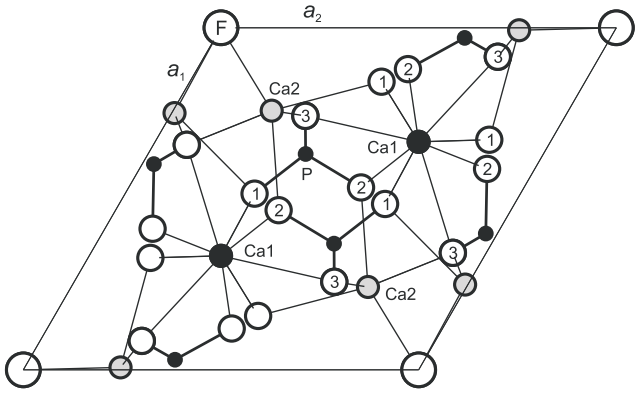

FIG 2 - Unit-cell contents of fluorapatite $[Ca1_4Ca2_6(PO_4)_6F_2$, Z = 1].

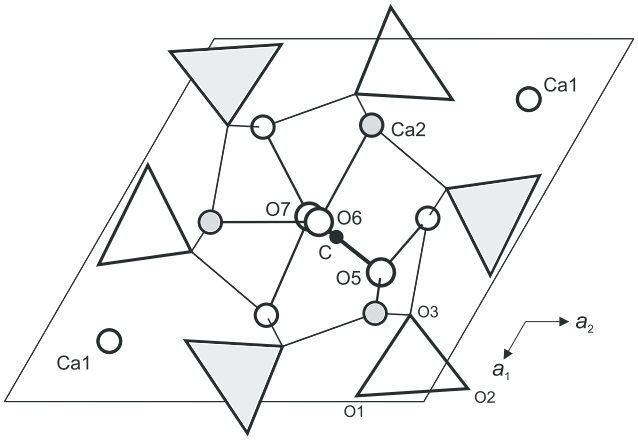

FIG 3 - Structure of hexagonal carbonate hydroxylapatite (CHAP), showing location of one of 12 possible orientations of A carbonate ion in apatite channel (six centred at z ≈ 0.5 and six at z ≈ 0.0 for $P6_3/m$ symmetry): unit-cell origin is in centre of figure; atoms of A carbonate ion are C, O5, O6 and O7; phosphate polyhedra are represented in the projection as triangles; shaded phosphate polyhedra and Ca2 atoms are centred at z = 3/4.

et al (1969) and Bonel (1972) usually cited as early pioneering studies. The FTIR spectra of the present high-pressure synthesised carbonate apatites are dominated by a complex band at about 1000 - 1100 cm^{-1} for the asymmetric stretch vibration of the phosphate group. The usual analytical bands for carbonate are the prominent doublet band at 1400 - 1600 cm^{-1} (asymmetric stretch vibration; ν_3) and the weak singlet band at 873 - 880 cm^{-1} (out-of-plane bend vibration; ν_2) (eg Figures 1 and 4). In addition, a weak band for the stretch vibration of structurally-bound OH may be present near 3572 cm^{-1}. Features consistent with the presence of the HPO_4^{2-} ion (Rey *et al*, 1991; Kim, Rey and Glimcher, 1996) are absent in the present spectra. Interpretation of the carbonate ν_3 band in the FTIR spectra of apatites with multiple carbonate species is complicated by band overlap and asymmetry of the doublet for the channel (type A) carbonate species (eg Fleet, Liu and King, 2004). Band overlap in the 1470 - 1450 cm^{-1} interval is particularly troublesome. Earlier studies on natural and synthetic Na-free CHAP (eg LeGeros *et al*, 1969; Bonel, 1972; Elliott, 2002; Fleet, Liu and King, 2004) found that type A carbonate was characterised by a doublet band at about 1545 and 1460 - 1450 cm^{-1} (ν_3) and a singlet band at about 878 cm^{-1} (ν_2), whereas type B carbonate has these bands at about 1450 - 1455, 1410 - 1420 and 871 cm^{-1}, respectively. However, in the present Na-bearing CHAP, CFAP and CCLAP crystals, which contain both A and B carbonate, the ν_3 doublet for type A

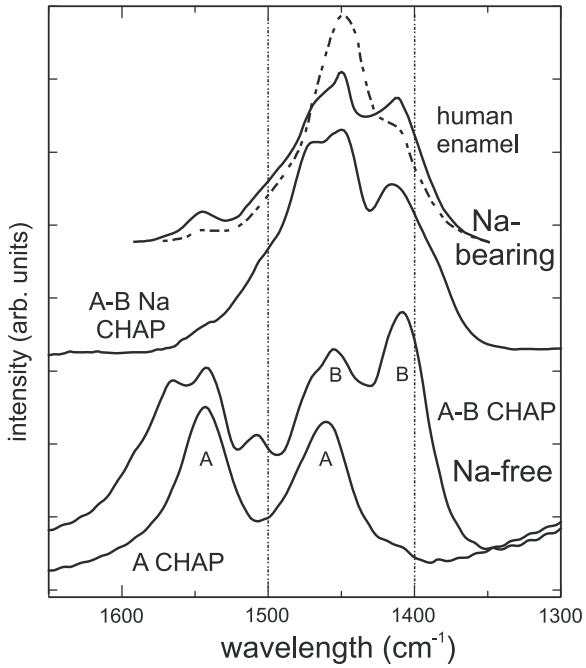

FIG 4 - Polarised IR spectra for human dental enamel (Elliott, 1994), compared with FTIR spectra for Na-free types A and A-B CHAP and Na-bearing type A-B CHAP; dashed spectrum of human enamel is polarised parallel to c-axis and continuous spectrum is polarised perpendicular to c-axis.

is seemingly shifted to lower wavenumber and into the region normally associated with type B carbonate (Fleet and Liu, 2007a, 2008a, 2008b; present Figure 4). The composite ν_2 band for these crystals has components for type A carbonate at 878 - 881 cm^{-1} and type B at 871 - 873 cm^{-1}, whereas for biological apatites this spectral region is normally deconvoluted to give singlet bands at 878 cm^{-1} (type A carbonate), 871 cm^{-1} (type B carbonate) and 866 cm^{-1} (labile carbonate; eg Rey *et al,* 1989, 1991).

Detection of carbonate by single-crystal X-ray diffraction

The refined structure parameters for a Na-bearing CHAP (LM005; Fleet and Liu, 2007a) are reproduced in Table 2. The oxygen atoms O5, O6 and O7 define the type A carbonate ion and O8 and O9 belong to the type B carbonate ion. Substitution of the carbonate ion into apatite is generally limited in extent and, unlike atom-for-atom solid solution, introduces new atomic positions. Although the Na cation, carbonate anion and vacancy substituents are disordered within the host Ca apatite structure, they are replicated in the average structure by the hexagonal $P6_3/m$ symmetry and therefore contribute coherent Bragg scattering intensity to the single-crystal diffraction pattern. The diffraction pattern represents a composite of the host structure and carbonate ions locally ordered in minimum energy locations and configurations. The atomic positions of the carbonate ions are resolved in residual electron density maps. However, because of the limited extent of substitution and high multiplicity of the carbonate atom positions, these residual peaks are usually very weak. In addition, atoms of the host structure are locally displaced to accommodate the carbonate ions, and this displacement results in anomalous increase in atomic displacement parameters (Leventouri *et al*, 2000, Fleet, Liu and King, 2004; present Figure 5). As a result of these problems, the X-ray structures of carbonate apatites present numerous challenges in interpretation, especially where carbonate contents are very low. In particular, electron densities that may be

TABLE 2

Positional and isotropic thermal parameters (Å^2) for average structure of CHAP (LM005).[1]

Position/ equipoint		Site occupancy	*x*	*y*	*z*	*U*
Ca1	4*f*	0.969(3)	2/3	1/3	0.0014(1)	0.0193(6)
Ca2	6*h*	0.987(2)	0.9875(1)	0.2499(1)	1/4	0.0181(4)
P	6*h*	0.871(7)	0.3691(2)	0.3977(2)	1/4	0.0145(7)
O1	6*h*	0.871(7)	0.4780(3)	0.3232(3)	1/4	0.0151(9)
O2	6*h*	1.0	0.4644(3)	0.5816(3)	1/4	0.0341(9)
O3	12*i*	0.903(8)	0.2556(3)	0.3395(3)	0.4263(3)	0.041(1)
C1	12*i*	0.083	0.046(1)2	0.065(1)	0.492(1)	0.025[3]
O5	12*i*	0.083	0.144(1)	0.220(1)	0.472(1)	0.025
O6	12*i*	0.083	0.005(1)	0.002(1)	0.662(1)	0.025
O7	12*i*	0.083	-0.010(1)	-0.028(1)	0.343(1)	0.025
O8	12*i*	0.064(4)	0.345(3)	0.424(3)	0.448(3)	0.025
O9	6*h*	0.129(8)	0.512(2)	0.361(2)	1/4	0.025

Notes:

1. Space group $P6_3/m$.
2. *x*,*y*,*z* for C1 to O7 from rigid body refinement.
3. U of C1 to O9 not refined.

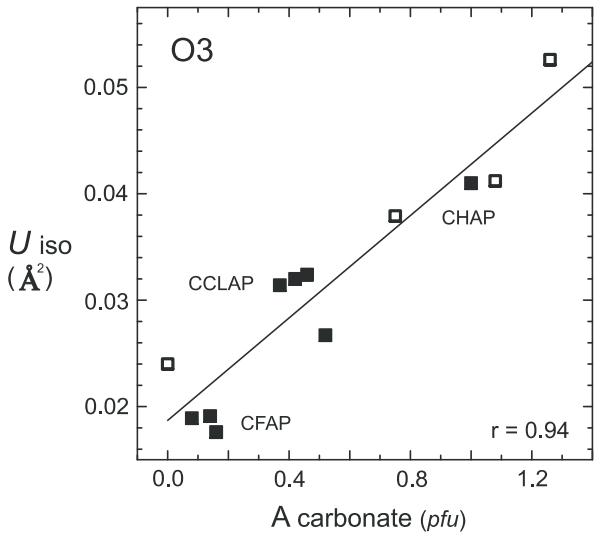

FIG 5 - Dependence of isotropic displacement parameter of O3 oxygen atom (U_{iso}) on amount of A carbonate in apatite channel: U_{iso} is the isotropic mean-square displacement of O3 resulting from the combined effects of thermal motion and structural disorder; note that A carbonate >1 represents second channel species (A2) of Na-free CHAP (open boxes); *pfu* is per formula unit.

appreciably less than that of a hydrogen atom and the overlap of carbonate and host-structure atoms limit the amount of structural information that can be extracted.

Location of type A carbonate ion

Resolution of the channel (type A) carbonate ion near the *c*-axis is complicated by high multiplicity and overlap of the electron density for the X anion(s), carbon atom, and two of the three carbonate oxygen atoms (cf Figure 3). For partial occupancy of the channel positions, it is not possible to refine independently the occupancy, positional and thermal parameters for these atoms. Fortunately, the channel was wholly occupied by carbonate in one sample of Na-bearing type A-B CHAP (LM005; Fleet and Liu, 2007a), and three-quarters occupied by carbonate in a Na-free type A CHAP (Fleet and Liu, 2003). For partial occupancy of the apatite channel, site occupancies may be determined with some confidence by refining the occupancy of the off-axis oxygen O5. The electron density for O5 is well resolved in residual electron density maps, at z = 0.5 for type A CHAP and at z = 0.0 and 0.5 for type A-B apatites, even in the Na-bearing CFAP structures that have less than 0.2 carbonate ions per unit cell (Fleet and Liu, 2008a).

Fleet and Liu (2003) found that the synthetic Na-free type A CHAP (PC71 in Table 1) had a new space group ($P\bar{3}$), and the carbonate ion was ordered along the apatite channel at z ≈ 0.5. A preferred structure for this $P\bar{3}$ type A CHAP was obtained by rigid body refinement of the channel carbonate ion, using a novel procedure for defining the ideal equilateral triangular geometry (Fleet and Liu, 2005), assuming the dimensions in calcite (eg O-O = 2.219 Å, C-O = 1.281 Å; Smyth and Bish, 1988). It was established that two of the oxygen atoms (O7 and O6) lay close to the *c*-axis at about $z \approx 0.333, 0.667$, consistent with a substitution mechanism controlled by charge balance requirements of:

$$[^{A}CO_3 = 2(OH)] \quad (1)$$

The carbonate ion is rotated about 11° counter-clockwise relative to the model structure of Figure 6a, and canted 9° away from the *c*-axis: note that it is viewed in Figure 6b in one of the six equivalent orientations present in electron density maps. The carbonate ion is located in the apatite channel by six bonds to Ca2 atoms, giving Ca2-O bond distances consistent with an ideal distribution of valence units for the carbonate oxygen atoms

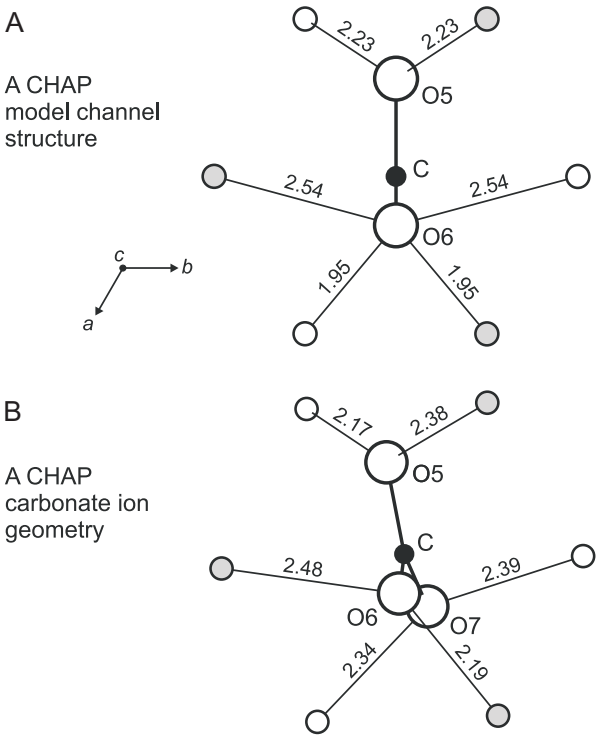

FIG 6 - Orientation of type A carbonate ion in apatite channel, viewed along *c*-axis: Ca2 cations are in channel wall at unit-cell heights of $z \approx 0.25$ (open circles) and $z \approx 0.75$ (shaded circles), and carbon atom (filled circle) is at $z \approx 0.5$: (A) model structure with Ca2 at 0.25 and 0.75 (shaded) and carbon at 0.5; (B) Na-free type A CHAP (PC71), showing carbonate ion rotated counter-clockwise and tilted away from the *c*-axis relative to model structure; bond distances are Å.

(ie 4/3 to C and 1/3 to 2 × Ca2). The phosphate groups are displaced slightly from ideal HAP positions to dilate the apatite channel in the immediate vicinity of the carbonate ion (at $z \approx 0.5$), and contract it above and below (ie at $z \approx 0.0, 1.0$).

The type A carbonate ion is located similarly in the channels of the Na-free and Na-bearing A-B CHAP (PC55, Fleet and Liu, 2004, 2005; LM005, Fleet and Liu, 2007a, respectively), but now rotated clockwise, opposite to the rotation for the type A CHAP (Figure 6b). The carbonate ion is rotated about 8° and canted 7° relative to the *c*-axis in the Na-free CHAP (PC55). In the Na-bearing A-B CHAP (LM005) it is rotated a similar amount (9°) but canted only <1°, as shown in Figure 3. These data were obtained for both structures by rigid body refinement of the carbonate ion, following the procedure of Fleet and Liu (2005). The orientations observed in our synthetic apatites are similar to those for channel carbonate ions in defect structures calculated using static lattice DFT (Peeters *et al*, 1997) and energy minimisation/molecular dynamics (Peroos, Du and de Leeuw, 2006) methods, except that the axial oxygen atoms (O6 and O7) are more-or-less symmetrically positioned with respect to $z \approx 0.0$ and 0.5 in our studies. The lack of significant canting and the symmetrical positioning of the carbonate ion in the apatite channel of the Na-bearing A-B CHAP reflects the absence of other channel constituents; the occupancy of the type A carbonate in this carbonate apatite being essentially 1.0. In comparison, carbonate ions were in competition with hydroxyl ions (and possible H_2O, as well) in the *c*-axis channels of the Na-free A (Fleet and Liu, 2003) and A-B CHAP (Fleet and Liu, 2004; Fleet, Liu and King, 2004) apatites.

The channel carbonate of the Na-bearing A-B CHAP (LM005) is displaced to one side of the apatite channel, with O6 and O7 lying almost on the *c*-axis and O5 extending outwards close to the channel wall and very close (1.14 Å in the average structure) to an O3 atom of a substituted phosphate group. The O6 oxygen is now close (2.45 Å) to a Ca2 cation at z = 0.75; the comparable O6-Ca2 distances in PC55 and the model structure of Figure 6a are 2.68 Å and 2.98 Å, respectively. In comparison, in Na-free type A CHAP the carbonate ion is more centrally located, resulting in O5-O3 distances of 2.07 and 2.24 Å.

The $P\bar{3}$ structure of type A CHAP (Fleet and Liu, 2003) provides a key piece of evidence for understanding the local environment of the channel carbonate ion in complex A-B apatites. In these disordered structures, the apatite channel must be dilated in the vicinity of the bulky carbonate ion and contracted above and below it at ($z \pm 0.5$). The anisotropic displacement parameters of O1, O2 and O3 for the average structures show that this is achieved largely by rotation of the PO_4 tetrahedron about the O1-P bond axis (Fleet, Liu and King, 2004).

In Na-free A-B CHAP synthesised at high pressure, there is also evidence of a second location for type A carbonate in a stuffed channel position (labelled A2 in Fleet and Liu, 2004; Fleet, Liu and King, 2004). An interesting feature of the structure of Na-bearing A-B CCLAP, in which carbonate competes with chlorine for the channel sites, is that the electron density for chlorine is not centred at the hexagonal end-member positions of $z = \pm$ (0.432, 0.068), but is spread out along the *c*-axis (Fleet and Liu, 2008b). Evidently chlorine is readily displaced by the introduction of the bulky carbonate ion.

Location of type B carbonate ion

Interpretation of the location of the B carbonate ion is more problematical, and has been controversial (Leventouri *et al*, 2000; Wilson *et al*, 2004; Fleet and Liu, 2004, 2007a, 2008a, 2008b). Logically, the B carbonate ion is located in the vicinity of the substituted phosphate group and occupies as many of the phosphate oxygen sites as possible. Several studies have noted that the presence of B carbonate is indicated by significant reduction in the occupancy of the P position (Wilson *et al,* 1999; Leventouri *et al*, 2000; Morgan *et al*, 2000). Indeed, for the Na-bearing apatites, the phosphorus occupancy decreases systematically with increase in total carbonate content through the series CFAP, CCLAP and CHAP. Also, our various studies have failed to detect any significant residual electron density in the vicinity of the phosphate group except for that associated with oxygen atoms of B carbonate lying close to sloping (ie inclined to *c*-axis) faces of the substituted phosphate tetrahedron (Fleet and Liu, 2004, 2007a). In addition, the B carbon atom of CHAP precipitated from aqueous solution was located in the centre of the sloping faces in the neutron scattering study of Wilson *et al* (2004). Further indirect evidence is that the coupling of A and B carbonate ions discussed below requires the omission of one of the two symmetry-related O3 atoms. In summary, the most likely location for the B carbonate ion in type A-B carbonate apatites is close to the sloping faces.

A preliminary location for the B carbonate ion in the present high *P-T* synthesised apatites was obtained from study of Na-free A-B CHAP in the form of residual electron density near O3 (Fleet and Liu, 2004; Fleet, Liu and King, 2004). This identified a probable B carbonate oxygen atom, which is presently labelled O8 (Figure 7a). The other two oxygen atoms were assumed to be buried in the electron density of O1 and O2. The X-ray structure of the Na-bearing CHAP (LM005; Fleet and Liu, 2007a; present Table 2) resulted in a similar orientation for the B carbonate ion, but now O9 is resolved separately from O1 in the average structure (Figure 6a). This structure confirmed that the B carbonate ion in CHAP is located near a sloping face of the substituted phosphate tetrahedron but inclined at an angle of 53° to the mirror plane; ie tilted 18° away from the sloping face.

The B carbonate ion is orientated similarly in Na-bearing CCLAP (Fleet and Liu, 2008b). However, in Na-bearing CFAP it is more closely parallel to the sloping faces of the substituted phosphate tetrahedron, being inclined at an angle of only 3.5° (Figure 7b). The mean O-O distances for representative structures

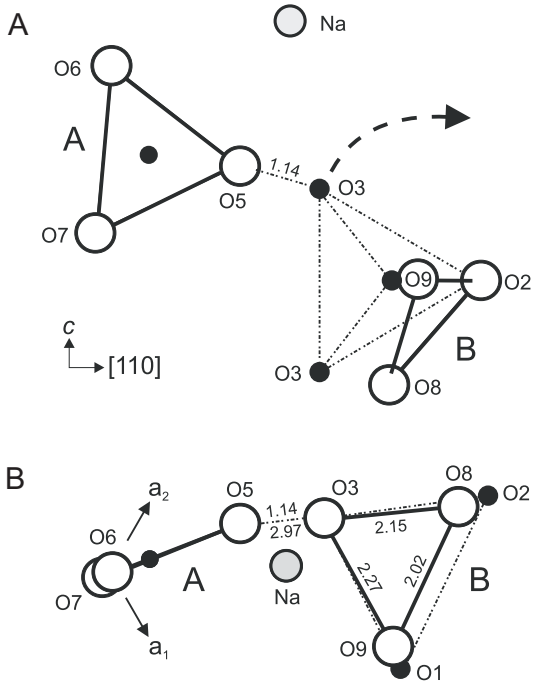

FIG 7 - Fragments of the structures of carbonate apatites, showing location of B carbonate ion close to the sloping faces of substituted phosphate tetrahedron: multiplicities due to $P6_3/m$ symmetry of the host apatite structure are not shown: (A) CHAP (and CCLAP), elevation view; (B) CFAP, c-axis projection; interatomic distances are in Å.

of these three composition series (X = OH, F, Cl) are 2.21, 2.15 and 2.33 Å for CHAP, CFAP and CCLAP, respectively. Discrepancies with the ideal O-O distance (2.219 Å) represent errors in locating atom positions in structures determined at the lower limit of resolution of the X-ray structure method using conventional laboratory equipment and do not imply that the carbonate ion geometries are anomalously distorted. It is emphasised that there is some ambiguity in defining the precise positions of B carbonate oxygen atoms located very close to phosphate oxygen atoms, since electron densities extensively overlap in the average structures.

The present location and orientation of the B carbonate ion in CFAP crystallised at high temperature and pressure is at variance with the conclusion of Leventouri *et al* (2000, 2001) and Antonakos, Liarokapis and Leventouri (2007), who proposed that the B carbonate was located on the (horizontal) mirror plane, with oxygen atoms at O1, O2 and a third location mid-way between the two symmetry related O3 atoms of the substituted phosphate group. Their conclusions were based on Rietveld neutron powder diffraction study of francolite from Epirus, Greece and its heat-treated products, as well as shifts in the ν_{3c} asymmetric stretching band of phosphate and lattice dynamics calculations. Their structure refinements did not yield direct evidence of the B carbonate ion, but there was indirect evidence from systematic change in anisotropic displacement parameters as a function of temperature, and change in P-O bond lengths for the average structure, in that P-O1 and P-O2 decreased with substitution of phosphate by carbonate and P-O3 increased. The P-O distances for the CFAP crystals in Fleet and Liu (2008a) do not show this trend; rather, P-O2 and P-O3 actually increase and decrease, respectively, relative to Durango fluorapatite (Hughes, Cameron and Crowley, 1989). Also, residual electron density consistent with the third carbonate oxygen on the mirror plane was absent in both this study and Leventouri *et al* (2000). It is well known that oxygen positions are determined with poor precision in conventional Rietveld powder structure refinement of apatites (eg White *et al*, 2005; Mercier *et al*, 2005). Our studies emphasise the unique advantage of single crystal diffraction methods in locating weak electron densities.

However, the relevant experimental observations in Leventouri *et al* (2000) and Fleet and Liu (2008a) are not significantly discrepant, since both studies found that O1 and O2 are shifted on the mirror plane toward the centre of the phosphate tetrahedron. The neutron powder diffraction study of Leventouri *et al* (2000) simply detected the average position of O1 and O2 in the annealed francolite structure, whereas Fleet and Liu (2008a) resolved separate O1/O9 and O2/O8 positions for the phosphate and carbonate oxygen atoms. They found that substitution by type B carbonate results in observed atom shifts of 0.31 Å for O1 to O9 and 0.41 Å for O2 to O8. When these shifts are weighted by the proportion of type B carbonate estimated for the Epirus francolite (0.95 *pfu*), the corresponding apparent shortening of the P-O1 and P-O2 bond lengths in the average structure is calculated to be about 0.05 and 0.06 Å, which compares favourably with about 0.04 and 0.04 Å, respectively, in Leventouri *et al* (2000).

Site occupancies and substitution mechanisms

Site occupancies for the A and B carbonate ions were obtained from the single-crystal X-ray structure refinements, and are summarised in Table 1 as formula amounts (Z = 1). The occupancy of the off-axis oxygen O5 was refined for the type A carbonate in Na-free CHAP and Na-bearing CFAP and CCLAP. The channel was assumed to be fully occupied by carbonate in Na-bearing CHAP LM005 and the carbon atom occupancy was refined for Na-bearing CHAP LM006. The B carbonate site occupancies for all of these structures are based on the refined occupancy of phosphorus; ie (6-P). Note that the Na contents in Table 1 were determined independently by electron probe microanalysis. In addition, the proportions of A and B carbonate from the X-ray structures are supported by agreement with the corresponding relative areas of the A and B ν_2 bands in FTIR spectra (Table 1; Figure 8): the A band is located at 878 - 881 cm^{-1} and the B band at 871 - 873 cm^{-1}. Although the ν_3 bands were used for estimating A/B site occupancies in synthetic Na-free A-B CHAP (Fleet and Liu, 2004; Fleet, Liu and King, 2004), this spectral region is not readily deconvoluted for Na-bearing carbonate apatites (see discussion below). Because the X-ray structure method yields absolute values for site occupancies, Figure 8 is the first independent verification of the ν_2 band method for estimating relative proportions of A and B carbonate in apatites. Moreover, the data in Figure 8 clearly show that Na promotes the entry of B carbonate into apatite.

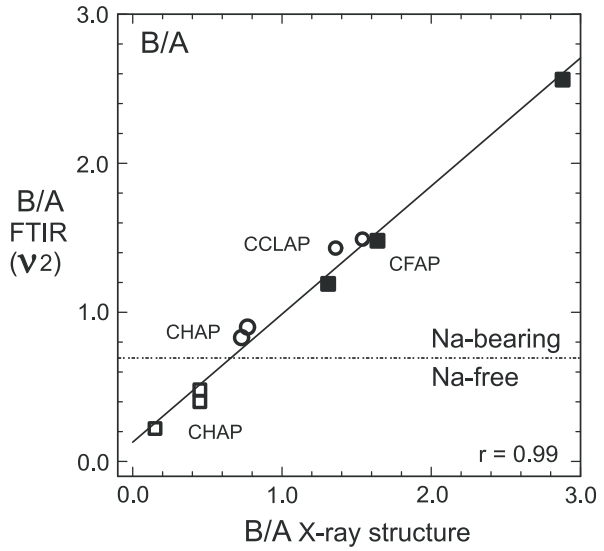

FIG 8 - Comparison of ratio of formula amounts of B and A carbonate determined by FTIR and X-ray structure methods. Note that Na promotes relative enrichment in B carbonate, consistent with substitution mechanism 2: open squares are Na-free CHAP; open circles are Na-bearing CHAP and CCLAP (as labelled); filled squares are Na-bearing CFAP.

The ratio of Na to A and B carbonate (Na:A:B) is approximately 1:1:1 in CHAP, 1:1:1.5 in CCLAP, and 1:1:(1.5 - 2) in CFAP (Table 1), and apparently is characteristic of each composition series. These correlations are consistent with the following substitution schemes for B carbonate:

$$[Na + {}^{B}CO_3 = Ca + PO_4] \quad (2)$$

and:

$$[0.5\,\square + {}^{B}CO_3 = 0.5Ca + PO_4] \quad (3)$$

which result in a complex substitution formula of $Ca_{10-(y+z)}Na_y\,\square_z[(PO_4)_{6-(y+2z)}(CO_3)_{y+2z}][X_{2-2x}(CO_3)_x]$, with $x \approx y \leq 1$, $z \approx 0$ for CHAP, $x \approx y \approx 4z \approx 0.4$ for CCLAP, and $x \approx y \approx 2z \approx 0.1$ for CFAP.

Sodium and vacancies at Ca sites are required for charge balancing the carbonate-for-phosphate substitution after the removal of the fourth oxygen anion. The correlation of Na with B and A carbonate in CHAP and with B/(1.5) and A in CCLAP, and B/2 and A in CFAP (Table 1) confirms that Na has an active role in the substitution of carbonate into these apatites. Thirdly, in the absence of a proximal B carbonate ion, the off-axis oxygen (O5) of the channel carbonate would be only about 1.1 - 1.2 Å

from an O3 oxygen atom of a phosphate group (Figure 7). These three factors strongly suggest that the A and B carbonate ions and Na are locally coupled in the structures of these apatites, to facilitate charge compensation and minimise the effects of spatial accommodation. The prohibitively short O5-O3 interaction is eliminated when the O3 oxygen atom in question is removed entirely from the structure and, logically, charge balance requirements favour placing the Na cation closest to this vacant O3 oxygen site. An explanation for the near-linear 1:1 correlation between Na and A carbonate (Table 1) is not intuitively obvious in the absence of a role for spatial accommodation, because Na is introduced to charge balance the introduction of B carbonate (substitution mechanism 2), but is not formally required to charge balance the A carbonate in substitution mechanism 1 [ie $^{A}CO_3 = 2X$].

The FTIR spectra (eg Figure 1) independently confirm that the A and B carbonate ions and Na are coupled locally as a defect cluster as depicted in Figure 7. We have noted above that the ν_3 bands of type A carbonate in Na-bearing carbonate apatites are shifted to lower wavenumber and extensively overlap the spectrum of type B carbonate. The resulting characteristic ν_3 band profile is similar for all Na-bearing carbonate apatite composition series (X = OH, F, Cl) and carbonate contents investigated (Fleet and Liu, 2007a, 2008a, 2008b). This consistency shows that the chemical environments of the Na cation and A and B carbonate ions are similar in all of these apatites: ie these substituents are present as a defect cluster common to all the composition series investigated (Table 1), and randomly distributed within the host apatite structures. It is possible that there exists a degree of intermediate range order, with several A-B pairs organised into columnar *c*-axis domains, analogous to the columnar domains suggested for mixed X anion occupancy in Ca apatites (Elliott, 2002; Wopenka and Pasteris, 2005). However, the X-ray diffraction patterns of these apatites do not reveal any evidence of extensive ordering and it seems unlikely that compositionally distinct domains analogous to those observed in Brazilian gem-grade apatite (Ferraris *et al*, 2005) exist in them. We recognise that charge compensation through the introduction of large cation site vacancies (substitution mechanism 3) may involve a separate defect cluster in CFAP and CCLAP, because both of these apatite series have molar (B/Na) > 1, although this is not reflected by change in their ν_3 band profiles (eg Figure 1).

Apatite biomineralisation

The present synthetic Na-bearing CHAP LM006 (with 3.5 wt per cent CO_2; Fleet and Liu, 2007a) has a similar composition to the inorganic fraction of bovine bone and human and pig dental enamel (Table 3) and its FTIR spectrum (B in Figure 1) is similar in the ν_3 region to that of rodent bone mineral (eg Rey *et al*, 1989; Aparicio *et al*, 2002) and dental enamel (Rey *et al*, 1991; Elliott, 2002; present Figure 4). All of these synthetic and natural materials are Na-bearing carbonate apatites, and their infrared spectra are characterised by ν_3 absorption more-or-less confined to the 1400 - 1500 cm^{-1} spectral interval. Therefore, the structure of CHAP LM006 is probably a good approximation to the local structure of carbonated hydroxylapatite in bone and enamel. An important result of our study is that the proportion of A and B carbonate in the synthetic Na-bearing CHAP samples (LM006 and LM005) has been determined independently of infrared spectroscopy using the single-crystal X-ray structure method, and shown to contain approximately equal amounts of A and B carbonate. In summary, we suggest that crystalline biological apatites appear to be Na-bearing type A-B carbonate hydroxylapatites, the mineral equivalent of LM006, with type A carbonate accounting for up to 50 per cent of total carbonate.

Earlier studies (eg Rey *et al*, 1991; Elliott, 2002) concluded that biological apatites were dominantly type B carbonate hydroxylapatites, based on the appearance of the ν_3 region IR bands. However, our recent studies show that the characteristic ν_3 region profile of biological apatites is the result of their Na content. The minor amount of Na in these apatites (Table 3) has a major influence on the IR spectra because it is concentrated in the defect clusters (Figure 7). It is not possible to deconvolute the ν_3 region of the FTIR spectra of Na-bearing CHAP and apatite biominerals without further crystal-chemical insight, and in any case the ν_3 region is often of limited utility for study of apatite extracted from bone because it tends to be obscured by absorption bands of functional groups on proteins and glucosaminoglycans (Rey *et al,* 1989). The weak and diffuse ν_3 region intensity beyond 1500 cm^{-1} (Figure 4) could represent multiple channel sites for carbonate ions. This explanation was tendered by Rey *et al* (1991) and is reinforced by the presence of a second channel carbonate species in Na-free CHAP (Fleet and Liu, 2004; Fleet, Liu and King, 2004), but is not supported by the X-ray structures for the synthetic Na-bearing CHAP. Alternative explanations for the smearing and displacement of the ν_3 band intensity for the A carbonate are multiple large-cation (Ca2) configurations around a single A carbonate site, and destabilisation of the A carbonate ion by close proximity of the O5 oxygen atom to the apatite channel wall (Figure 3).

TABLE 3

Compositions of a synthetic Na-bearing carbonate apatite, inorganic fraction of bone and tooth enamel.

	Na-CHAP LM006 (wt %)	Bovine bone[1] (wt %)	Enamel[1] (wt %)
Ca	39.5	36.6	37.6
P	17.6	17.1	18.3
CO_2	3.5	4.8	3.0
Na	0.81	1.0	0.7
K	-	0.07	0.05
Mg	-	0.6	0.2
Sr	-	0.05	0.03
Cl	-	0.1	0.4
F	-	0.1	0.01

Note:

1. After Elliott (2002).

In contrast to the ν_3 region, the complex ν_2 band appears to better reflect the true proportions of the principal carbonate species in biological apatites, as we have demonstrated for the present synthetic apatites using the results of the single-crystal X-ray structure method for reference (Figure 8). Rey and coworkers reported B/A ratios from ν_2 region spectra ranging from 1.1 to 0.8 for pig enamel (Rey *et al*, 1991) and 1.4 to 1.2 for various bone samples (cow, human, chicken, rat and rabbit; Rey *et al*, 1989; Kim, Rey and Glimcher, 1996). Based on their ν_2 region spectra, these biological apatites are all type A-B carbonate hydroxylapatites.

Finally, we recognise that, although the overall structure of crystalline biological apatites appears to have been reproduced, the present synthetic CHAP crystals differ markedly from bone mineral in respect to crystal size, reactivity of the surface layer, and absence of HPO_4^{2-} (eg Rey *et al*, 1989; Kim, Rey and Glimcher, 1996; Boskey, 2003). Also, although the apatite species of bone is generally understood to be CHAP, structurally-bound hydroxyl is commonly not detected by spectroscopic studies (including infrared, Raman and nuclear magnetic resonance) on mineralised tissue extracted from bone (eg Wopenka and Pasteris, 2005). However, these null results are probably attributable to the procedures used for processing mineralised tissues from mammals (Aparicio *et al*, 2002; Cho, Wu and Ackerman, 2003). In several of our experiments on

CHAP, excess Na_2CO_3 in the starting mixture resulted in the incorporation of the hydrogen-carbonate (bicarbonate) ion in the *c*-axis structural channel (Fleet and Liu, 2007b). We reported that the hydrogen-carbonate ion is only loosely bound in the apatite channel, and breaks down on ageing at room temperature with loss of the volatile decomposition products CO_2 and H_2O. These observations point to a possible role for the apatite channel in mediating acid-base reactions in the body (cf Bushinsky *et al*, 2002), and help to explain why the channel constituents of the nanoscale crystals of hydroxylapatite in bone are labile.

ACKNOWLEDGEMENTS

We thank a reviewer for helpful comments, Michael Jennings for collection of X-ray reflection data, Penny King for use of FTIR equipment, and the Natural Sciences and Engineering Research Council of Canada for financial support.

REFERENCES

Antonakos, A, Liarokapis, E and Leventouri, T, 2007. Micro-Raman and FTIR studies of synthetic and natural apatites, *Biomaterials*, 28:3043-3054.

Aparicio, S, Doty, S B, Camacho, N P, Paschalis, E P, Spevak, L, Mendelsohn, R and Boskey, A L, 2002. Optimal methods for processing mineralized tissues for Fourier transform infrared microspectroscopy, *Calcif Tissue Int*, 70:422-429.

Bonel, G, 1972. Contribution à l'étude de la carbonatation des apatites. I. Synthèse et étude des propriétés physico-chimiques des apatites carbonatées du type A, *Annales de Chimie (*Paris), 7:65-88.

Boskey, A L, 2003. Mineral analysis provides insights into the mechanism of biomineralization, *Calcif Tissue Int*, 72:533-536.

Bros, R, Carpena, J, Sere, V and Beltritti, A, 1996. Occurrence of Pu and fissiogenic REE in hydrothermal apatites from the fossil nuclear reactor 16 at Oklo (Gabon), *Radiochim Acta*, 74:277-282.

Brudevold, F, Gardner, D E and Smith, F A, 1956. Distribution of fluorine in human enamel, *J Dental Res*, 35:420-429.

Bushinsky, D A, Smith, S B, Gavrilov, K L, Gavrilov, L F, Li, J and Levi-Setti, R, 2002. Acute acidosis-induced alteration in bone bicarbonate and phosphate, *Am J Physiol-Renal Physiol*, 283:F1091-F1097.

Cho, G, Wu, Y and Ackerman, J L, 2003. Detection of hydroxyl ions in bone mineral by solid state NMR spectroscopy, *Science*, 300:1123-1127.

Elliott, J C, 1994. *Structure and Chemistry of the Apatites and Other Calcium Orthophosphates*, 389 p (Elsevier: Amsterdam).

Elliott, J C, 2002. Calcium phosphate biominerals, in *Phosphates: Geochemical, Geobiological and Material Importance*, *Reviews in Mineralogy and Geochemistry, 48* (eds: M J Kohn, J Rakovan and J M Hughes), pp 427-453 (Mineralogical Society of America: Washington).

Ferraris, C, White, T J, Plévert, J and Wegner, R, 2005. Nanometric modulation in apatite, *Phys Chem Mineral*, 32:485-492.

Fleet, M E and Liu, X, 2003. Carbonate_apatite type A synthesized at high pressure: New space group (*P*3*)* and orientation of channel carbonate ion, *J Solid State Chem*, 174:412-417.

Fleet, M E and Liu, X, 2004. Location of type B carbonate ion in type A-B carbonate apatite synthesized at high pressure, *J Solid State Chem*, 177:3174-3182.

Fleet, M E and Liu, X, 2005. Local structure of channel ions in carbonate apatite, *Biomaterials*, 26:7548-7554.

Fleet, M E and Liu, X, 2007a. Coupled substitution of type A and B carbonate in sodium-bearing apatite, *Biomaterials*, 28:916-926.

Fleet, M E and Liu, X, 2007b. Hydrogen carbonate ion in synthetic high-pressure apatite, *Am Mineral*, 92:1764-1767.

Fleet, M E and Liu, X, 2008a. Accommodation of the carbonate ion in fluorapatite synthesized at high pressure, *Am Mineral*, in press.

Fleet, M E and Liu, X, 2008b. Type A-B carbonate chlorapatite synthesized at high pressure, *J Solid State Chem*, accepted.

Fleet, M E, Liu, X and King, P L, 2004. Accommodation of the carbonate ion in apatite: An FTIR and X-ray structure study of crystals synthesized at 2-4 GPa, *Am Mineral*, 89:1422-1432.

Harlov, D E, Foerster, H-J and Nijland, T G, 2002. Fluid-induced nucleation of (Y + REE)-phosphate minerals within apatite; nature and experiment, *Am Mineral*, 87:245-261.

Hughes, J M , Cameron, M and Crowley, K D, 1989. Structural variations in natural F, OH, and Cl apatites, *Am Mineral*, 74:870-876.

Hughes, J M and Rakovan, J, 2002. The crystal structure of apatite, $Ca_5(PO_4)_3(F,OH,Cl)$, in *Phosphates: Geochemical, Geobiological and Material Importance*, *Reviews in Mineralogy and Geochemistry, 48* (eds: M J Kohn, J Rakovan and J M Hughes), pp 1-12 (Mineralogical Society of America: Washington).

Ivanova, T I, Frank-Kamenetskaya, O V, Kol'tsov, A B and Ugolkov, V L, 2001. Crystal structure of calcium-deficient carbonated hydroxyapatite. Thermal decomposition, *J Solid State Chem*, 160:340-349.

Kim, H M, Rey, C and Glimcher, M J, 1996. X-ray diffraction, electron microscopy, and Fourier transform infrared spectroscopy of apatite crystals isolated from chicken and bovine calcified cartilage, *Calcif Tissue Int*, 59:58-63.

LeGeros, R Z, Trautz, O R, Klein, E and LeGeros, J P, 1969. Two types of carbonate substitution in the apatite structure, *Experimentia*, 25:5-7.

Leventouri, T, Chakoumakos, B C, Moghaddam, H Y and Perdikatsis, V, 2000. Powder neutron diffraction studies of a carbonate fluorapatite, *J Mater Res*, 15:511-517.

Leventouri, T, Chakoumakos, B C, Papanearchou, N and Perdikatsis, V, 2001. Comparison of crystal structure parameters of natural and synthetic apatites from neutron powder diffraction, *J Mater Res*, 16:2600-2606.

Mason, H E, Kozlowski, A and Phillips, B L, 2007. Solid-state NMR study of the role of H and Na in AB-type carbonate hydroxylapatite, *Chem Mater*, 20:294-302.

McClellan, G H and Lehr, J R, 1969. Crystal chemical investigation of natural apatites, *Am Mineral*, 54:1374-91.

Mercier, P H J, Le Page, Y, Whitfield, P S and Mitchell, L D, 2005. Geometrical parameterization of the crystal chemistry of *P63/m* apatite. II. Precision, accuracy and numerical stability of the crystal-chemical Rietveld refinement, *J Appl Crystallogr*, 39:369-375.

Morgan, H, Wilson, R M, Elliott, J C, Dowker, S E P and Anderson, P, 2000. Preparation and characterization of monoclinic hydroxyapatite and its precipitated carbonate apatite intermediate, *Biomaterials*, 21:617-627.

O'Reilly, S Y and Griffin, W L, 2000. Apatite in the mantle: Implications for metasomatic processes and high heat production in Phanerozoic mantle, *Lithos*, 53:217-232.

Pan, Y and Fleet, M E, 2002. Compositions of the apatite-group minerals: Substitution mechanisms and controlling factors, in *Phosphates: Geochemical, Geobiological and Material Importance*, *Reviews in Mineralogy and Geochemistry, 48* (eds: M J Kohn, J Rakovan and J M Hughes), pp 13-49 (Mineralogical Society of America: Washington).

Peeters, A, De Maeyer, E A P, Van Alsenoy, C and Verbeeck, R M H, 1997. Solids modeled by ab initio crystal-field methods. 12. Structure, orientation and position of A-type carbonate in a hydroxyapatite lattice, *J Phys Chem B*, 101:3995-3998.

Peroos, S, Du, Z and de Leeuw, N H, 2006. A computer modelling study of the uptake, structure and distribution of carbonate defects in hydroxyapatite, *Biomaterials*, 27:2150-2161.

Rey, C, Collins, B, Goehl, T, Dickson, I R and Glimcher, M J, 1989. The carbonate environment in bone mineral: A resolution-enhanced Fourier transform infrared study, *Calcif Tissue Int*, 45:157-164.

Rey, C, Renugopalakrishnan, V, Shimizu, M, Collins, B and Glimcher, M J, 1991. A resolution-enhanced Fourier transform infrared spectroscopic study of the environment of the CO_3^{2-} ion in the mineral phase of enamel during its formation and maturation, *Calcif Tissue Int*, 49:259-268.

Smyth, J R and Bish, D L, 1988. *Crystal Structures and Cation Sites of the Rock-Forming Minerals*, 332 p (Allen and Unwin: London).

Suetsugu, Y, Takahashi, Y, Okamura, F P and Tanaka, J, 2000. Structure analysis of A-type carbonate apatite by a single-crystal X-ray diffraction method, *J Solid State Chem*, 155:292-297.

White, T J, Ferraris, C, Kim, J and Madhavi, S, 2005. Apatite – An adaptive framework structure, in *Micro- and Meso-Porous Mineral Phases, Reviews in Mineralogy and Geochemistry, 57* (eds: G Ferraris and S Merlino), pp 307-373 (Mineralogical Society of America and the Geochemical Society: Washington).

Wilson, R M, Dowker, S E P and Elliott, J C, 2006. Rietveld refinements and spectroscopic structural studies of a Na-free carbonate apatite made by hydrolysis of monetite, *Biomaterials*, 27:4682-4692.

Wilson, R M, Elliott, J C and Dowker, S E P, 1999. Rietveld refinement of the crystallographic structure of human dental enamel apatites, *Am Mineral*, 84:1406-1414.

Wilson, R M, Elliott, J C, Dowker, S E P and Smith, R I, 2004. Rietveld structure refinement of precipitated carbonate apatite using neutron diffraction data, *Biomaterials*, 25:2205-2213.

Wopenka, B and Pasteris, J D, 2005. A mineralogical perspective on the apatite in bone, *Mater Sci Engin*, C25:131-143.